INTERNATIONAL ATOMIC ENERGY AGENCY
UNITED NATIONS EDUCATIONAL, SCIENTIFIC AND CULTURAL ORGANIZATION
INTERNATIONAL CENTRE FOR THEORETICAL PHYSICS
I.C.T.P., P.O. BOX 586, 34100 TRIESTE, ITALY, CABLE CENTRATOM TRIESTE

UNITED NATIONS INDUSTRIAL DEVELOPMENT ORGANIZATION

INTERNATIONAL CENTRE FOR SCIENCE AND HIGH TECHNOLOGY
(c/o INTERNATIONAL CENTRE FOR THEORETICAL PHYSICS 34100 TRIESTE (ITALY) VIA GRIGNANO, 9 (ADRIATICO PALACE) P.O. BOX 586 TELEPHONE 040-224572 TELEFAX 040-224575 TELEX 460449 APH I

H4.SMR/676-25

SECOND SCHOOL ON THE USE OF SYNCHROTRON RADIATION IN SCIENCE AND TECHNOLOGY:
"JOHN FUGGLE MEMORIAL"

25 October - 19 November 1993

Miramare - Trieste, Italy

EXAFS

A. Fontaine
L.U.R.E.
Orsay, France

III EXAFS

Model : single scattering of the photoelectron

Data analysis

Data Collection

Examples.

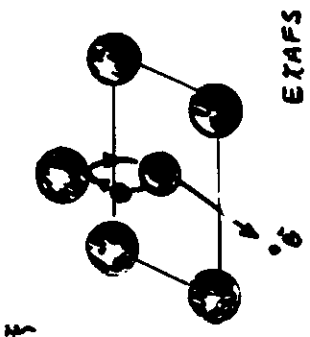

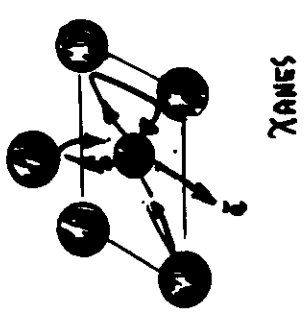

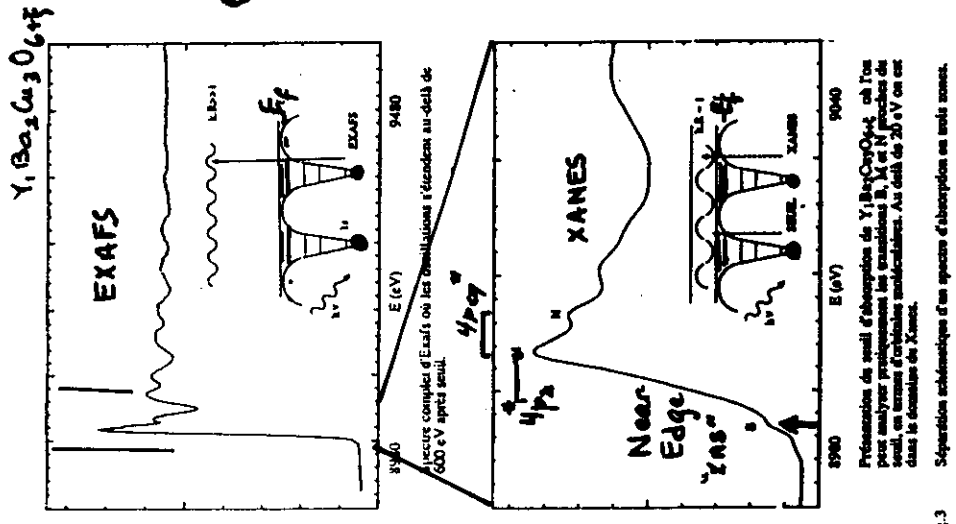

Fig.3 Séparation schématique d'un spectre d'absorption en trois zones.

Cu . Seuil K

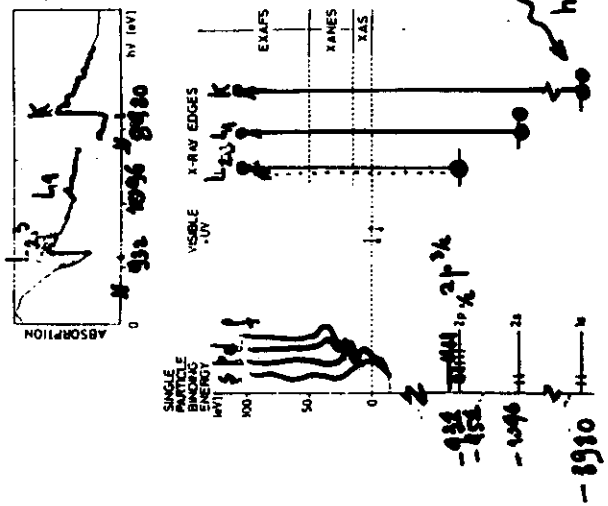

Fig.2 Description schématique des transitions optiques et des niveaux de cœur dans une image d'interaction à une particule (d'après tables J.Goulon-esrf-1999).

"Transition à une particule"

$$\mu \sim \sum_f |\langle f | \vec{R}.\vec{E} | i \rangle|^2 \, \delta(E_f - E_i + \hbar\omega)$$

$$|f\rangle = |f_0\rangle + \text{ondelette (réelle) de diffusion}$$

Règles de sélection $\Delta \ell_{i,f} = \pm 1 \quad \Delta m = 0$

III . 3

Heuristic derivation

$$\mu = \sum_f |\langle i | \vec{R}.\hat{\varepsilon} | f \rangle|^2 \, \delta(E_f - E_i - \hbar\omega)$$

ISOLATED ATOM

$$Y_{\ell,0}\left(\frac{\vec{R}}{R}\right) h_1^{\ell}(kR)\, e^{i\delta_\ell'(k)}$$

$$|f_0\rangle \sim \frac{e^{i(kR_j + \delta_i')}}{2kR_j}$$

≡ OUT GOING WAVE

~ plane wave @ R_j

SURROUNDED EMITTER

$$|f\rangle = |f_0\rangle \, (1 + \chi)$$

Back scattering

$$f_j(\pi, k) = \frac{1}{2ik} \sum_\ell (2\ell+1)(e^{2i\delta_\ell} - 1) P_\ell(-1)$$

Coming back on the central atom

$$\frac{e^{ikR_j}}{R_j} \; e^{i\delta_i(k)}$$

EXAFS SIGNAL for a

$$\chi(k) = \frac{\mu - \mu_0}{\quad} = \frac{-|f_j(\pi,k)|}{\quad} \sin(2kR_j + [2\delta_i' + \beta_j])$$

$$\chi(k) = \frac{\mu - \mu_0}{\mu_0}$$

$$\chi(k) = -\frac{1}{k} \sum_j \frac{1}{R_j^2} \left| f_j(\pi, k) \right| \sin\left(2k R_j + 2\delta_1(k) + \theta\right)$$

Powder or cubic lattice shell $\sum N_j$ $\times e^{-2\sigma_j^2 k^2}$ $\cdot e^{-\frac{R_j}{\lambda}}$

- $\frac{\hbar^2 k^2}{2m} = E - E_0$ origin of the kinetic energy
- $e^{-\frac{R_j}{\lambda}}$ mean free path of the photoelectron
- $e^{-2\sigma_j^2 k^2}$ D.W. static or dynamic disorder

ADVANTAGES of EXAFS.

(I) SELECTIVITY of the "ELECTRON" SOURCE

Cu K 8979.8 Zn K 9659 Eu L_{III} 6977 eV.

(II) GOOD ACCURACY IN BOND LENGTH DET

0.01 Å

(III) CHEMICAL IDENTIFICATION of NEIGHBORS & COORDINATION NUMBERS

ΔR large enough, $\pm 1/4$ in best cases (OUT of 12)

NEEDS

PHASE SHIFTS & BACKSCATTERING AMPLITUDES

III.3 c

DEBYE-WALLER DAMPING

Zn : 25 K

Zn : 300 K

-0.05 0.05 100 300 500 eV

Debaba Hermique croit avec le n° couche

Robe et al. : Ge, Cu Analyse avec $\theta_{Einstein}$

a = 2.66 Å c/a = 1.86

a = 2.912 Å

R_3 = 3.925 Å at 25 K. Crystallographic data

C. Jaggi, L. Tröger, J. Arvanitis, K. Baberschke

J. App. Phys (1993)

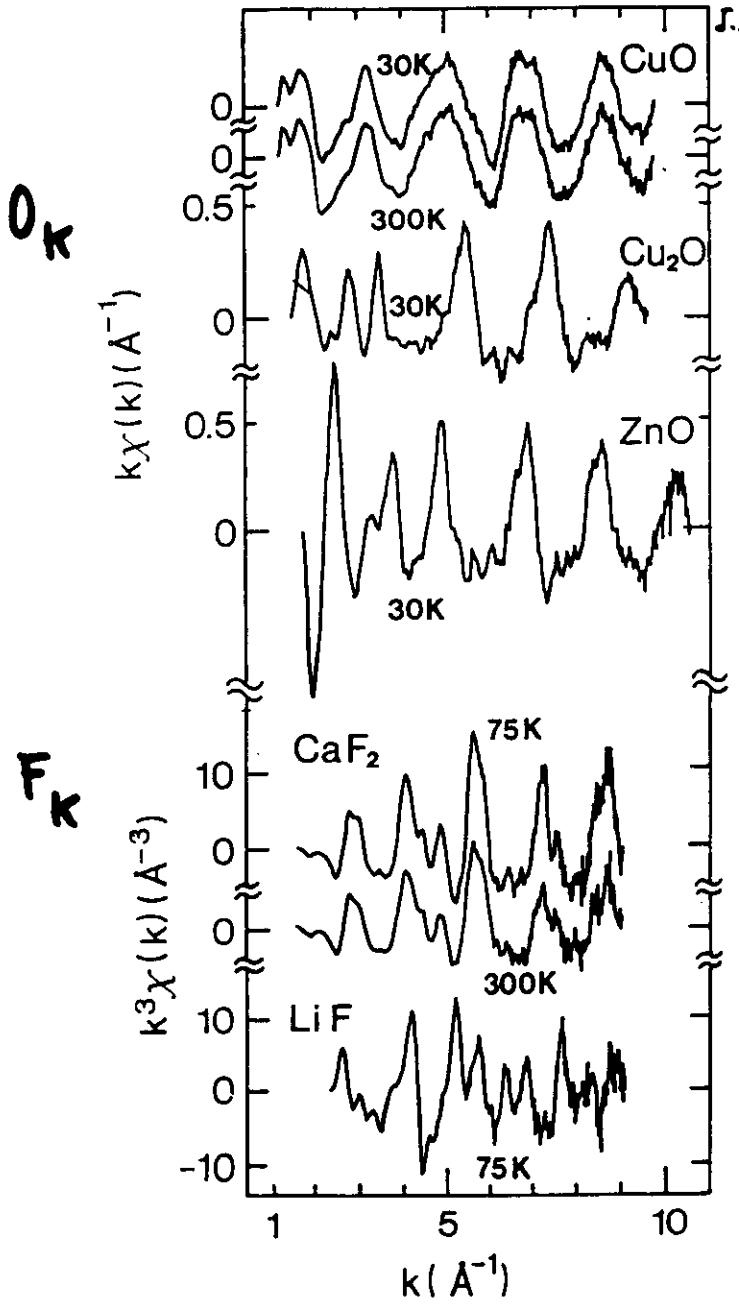

Fig. 3

III.3.b

Mean free path of the photoē

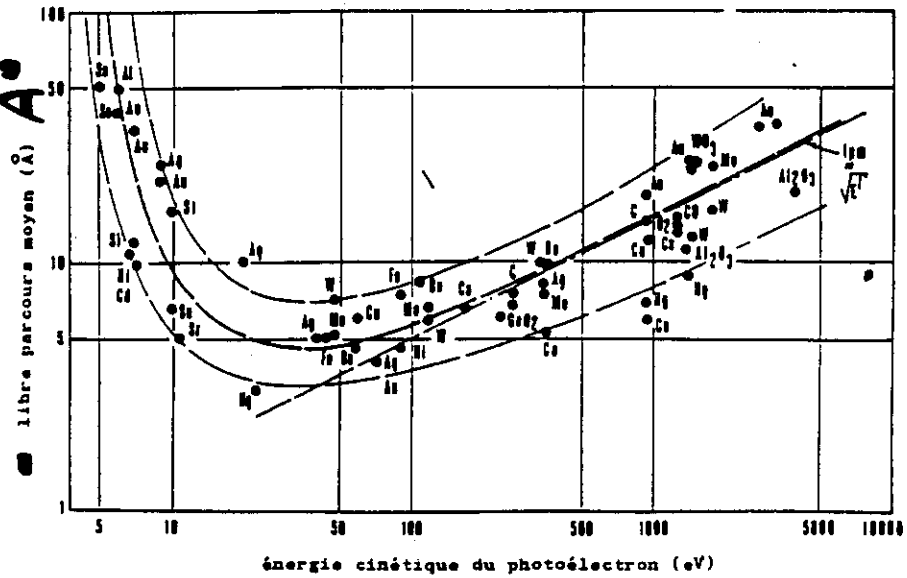

→ eV

$\lambda \propto k$

$E_{kin} > 50eV$

Figure I.6 - d'après C.R. Brundle (référence / 3 /).
Libre parcours moyen des électrons dans un solide en fonction de leur énergie cinétique.

"universal" ?

$\lambda \sim k$ a.u.

. *The lro-sro controversy*

Along the previous sections, we have described the debate that occurred between the supporters of the l.r.o. (long-range order) and s.r.o. (short-range order) theories. the rôle of the immediate surroundings in XAFS: We could cite Hanawalt (1932): "While it is true that the structure shown by vapors differs in details from that displayed by the same substance in the solid state, yet the outstanding observation is the high degree of similarity between them. This fact probably means that the same explanation should be applicable to both of them." or Coster (1935):

"As has been shown in several papers from this laboratory, the fine structure of X-ray absorption edges, in accordance with Kronig's theory, is intimately related to the type of crystal lattice in which the absorbing element occurs. Besides, however, it has been demonstrated that the immediate surrounding in the crystal lattice of the atoms in question is also of great importance."

92-55

SUMMARY

EXAFS ≃ SPHERICAL LEED

≃ DIFFRACTION OF LOW ENERGY ELECTRON

where the SOURCE OF $\vec{e}$ IS INSIDE THE SAMPLE ON A SELECTED ATOM

EXAFS and OTHER SCATTERING TECHNIQUES

- X-RAY SCAT. PAIR CORRELATION . FUNCT. Bimodality AA / AB / BB
- Bad News EXAFS does not see long distances
- Good News EXAFS is accurate to evaluate local ORDER
- NEUTRONS $b_{Ni} \gg b_{Co}$ GOOD CONTRAST
- EXAFS $f_t(\pi, k)$ of ± PHASE
- X-Ray . WEAKER INTERACTION THAN $\vec{e}$ STRONGER ___ THAN n
- Hard X-rays Sample "REASONABLE VOLUME"

SUCCESS
1934
W. HARTREE, D. HARTREE

Self consistent calculations of the wave functions to test Kronig & Penney's model with a machine made of 20 bunches of needles

Gally: checked Kr. graph oscillation and reported "The discrepancy could be removed by assuming Q_{GeCl} at 2.07 Å instead of (2.10±0.08) as known after WIERL" Actual value is 2.08 Å !!!

Coster, Kramer $AsCl_3$ same success after modern recalculation

Moseley (1913) Emission lines K_α, K_β Ca → Zn

IX-4 - Fine Structure, Kronig Oscillations

Fine structure in SOLID Successful evaluation of the fine Asymmetry.

Fe bcc

Fe in alloy Fe Ni

Ni

Veldkamp (1933)

III.1

or Smoluchowski, struck by the analogy between the spectra

of bulk copper and disordered $AuCu_3$ (1935b): "Die Erklärung dieser Tatsache ist darin zu suchen, daß die in der Theorie gebrauchten Approximationsmethoden und der Begriff einer Braggschen Reflexion in diesem Energiegebiet der herausgeworfenen Elektronen nicht mehr brauchbar sind, und daß, wie öfters betont, die Schwankungen des Absorptionskoeffizienten hier mehr durch Atom- als durch Gittereigenschaften verursacht sind (The explanation of this fact must be sought, that the approximation method and the concept of Bragg reflection required by the theory is no longer necessary in that domain of the photoelectron energy, and that, as often stressed, the absorption coefficient structures depend here more on the atomic than on the lattice characteristics)." Strangely enough, this controversy was the opposition of two theories which were originally conceived by the same man.

Krönig

III.5 DATA ANALYSIS

a/ SCHEME

$\Delta E_0 = E_0 - E_{threshold}$

$\frac{\hbar^2 k^2}{2m} = E - E_0$

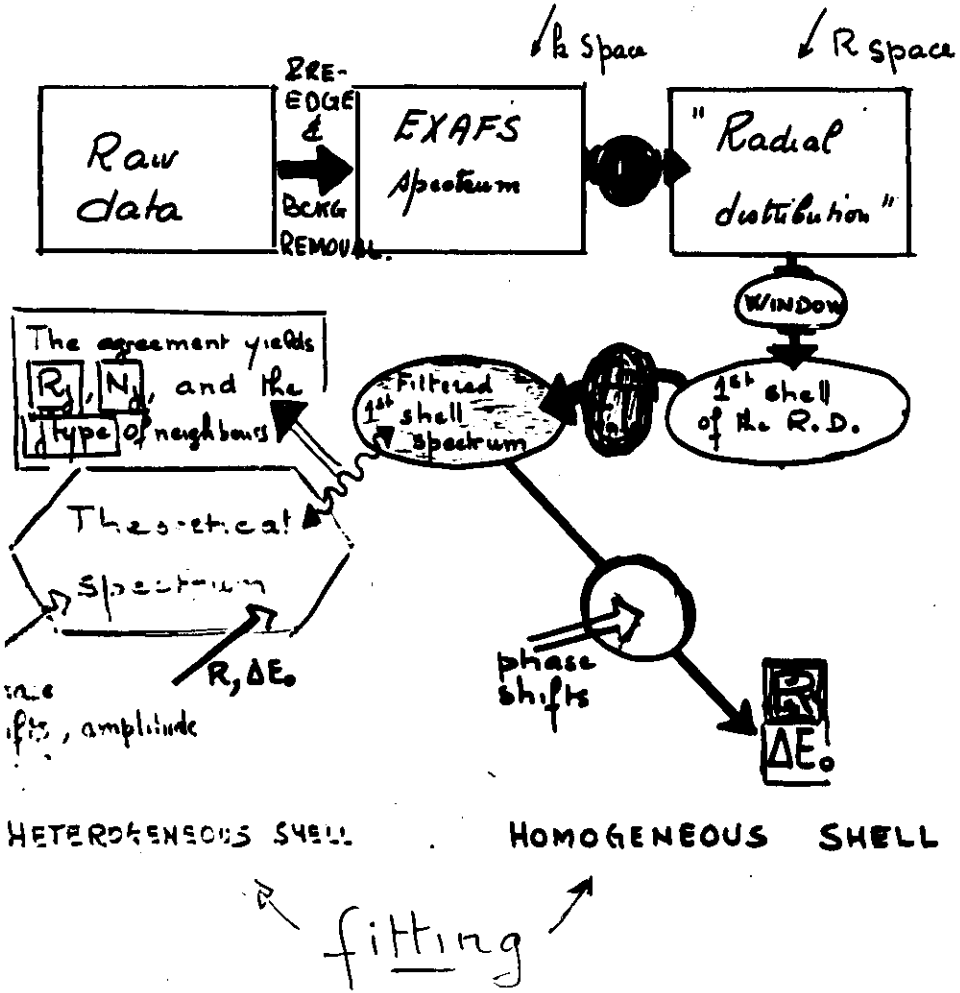

Hypothetic compounds

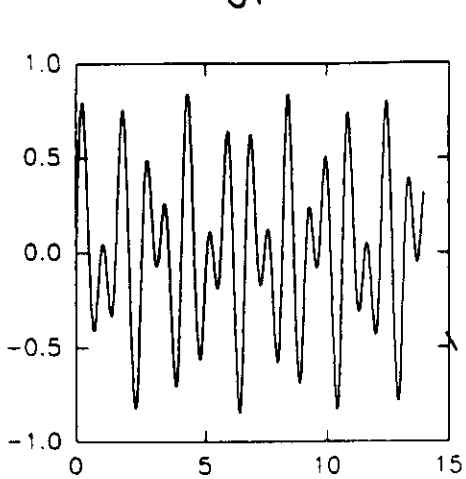

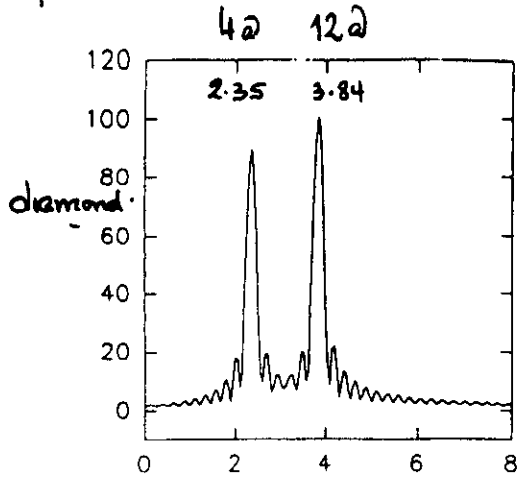

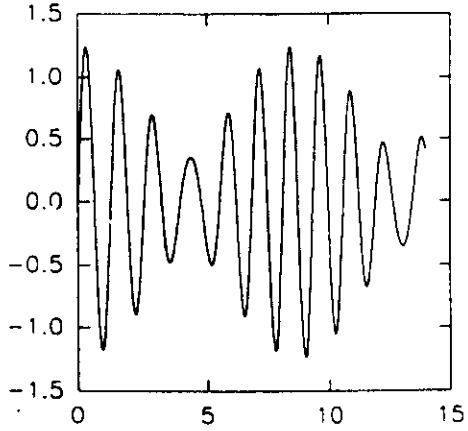

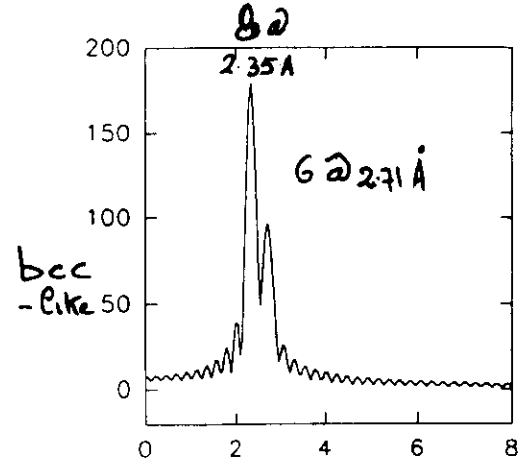

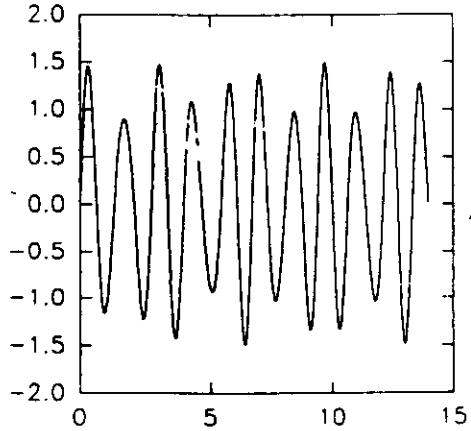

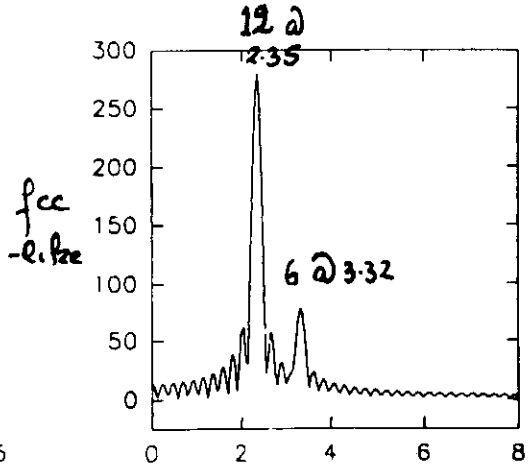

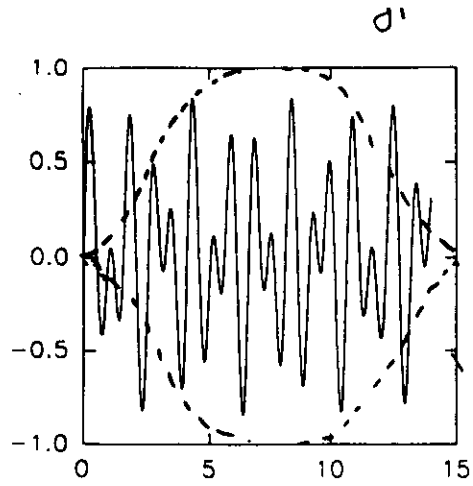

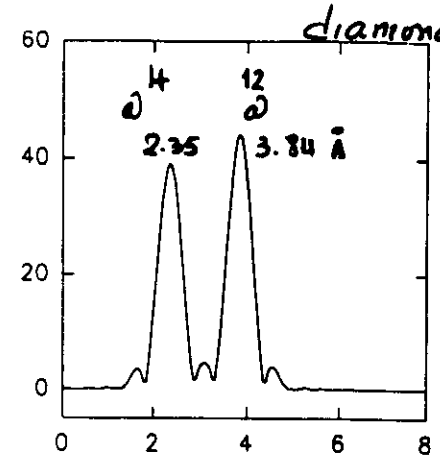

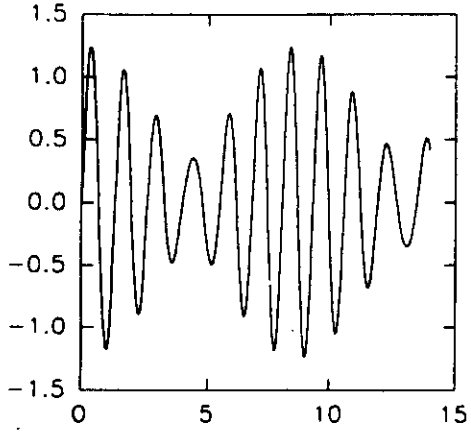

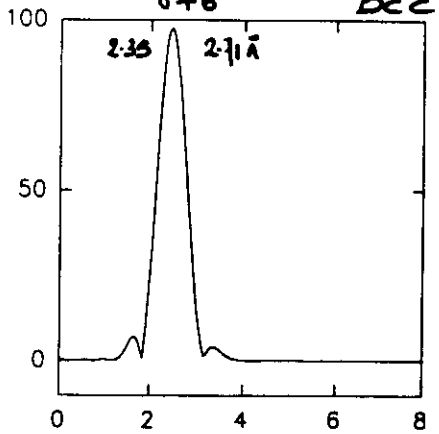

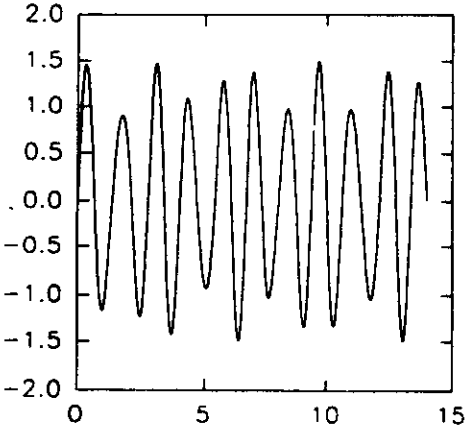

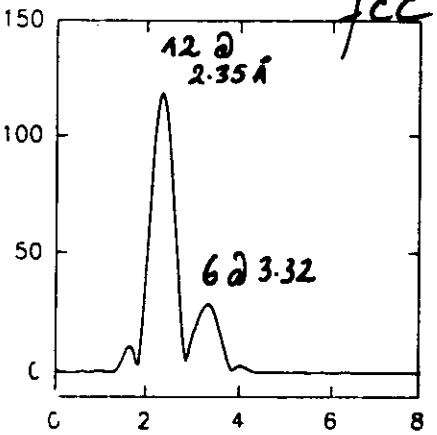

III S.2 Phase shifts & amplitudes

* Theoretical evaluations

  Excellent for phase shifts

  Not that GOOD for AMPLITUDES

* Best procedure: to evaluate + for the AB pair (Absorber → Backs)

  a/ Measure a well-known sample
  with a simple lattice
  with a structure close to the
  UNKNOWN sample
  with **A** as absorber
  B as backscatterer

  b/ Extract phase shift $+(k)$
  and amplitudes $|f(\pi), R|$

  c/ Transfer into the data analysis
  of the unknown sample.

* KEEP STANDARDS & INVESTIGATED SAMPLES AS CHEMICALLY CLOSE AS POSSIBLE

* WELL-CONDITIONNED PROBLEM

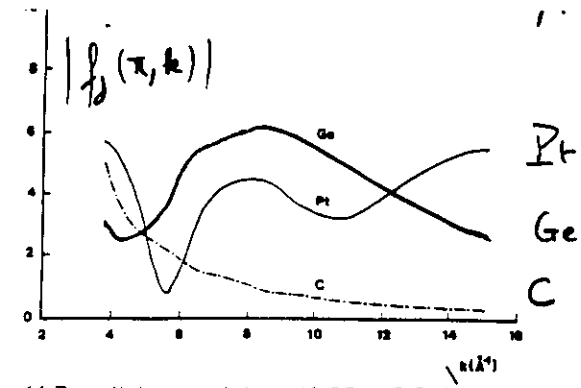

ure 6.4. Theoretical backscattering amplitudes versus k for C ($Z = 6$), Ge ($Z = 32$), and Pt ($Z = 78$) after Teo and Lee (14).

Pt
Ge
C

f amplitudes

Total phase

$2kR_j + \phi(k)$

$\phi(k) = 2\delta_1(k) + \theta_j(k)$

- $\left\langle \frac{1}{2}\frac{d\phi(k)}{dk} \right\rangle \lesssim 0.40$

low Z elements

high Z: $\phi(k)$ non monotonous.

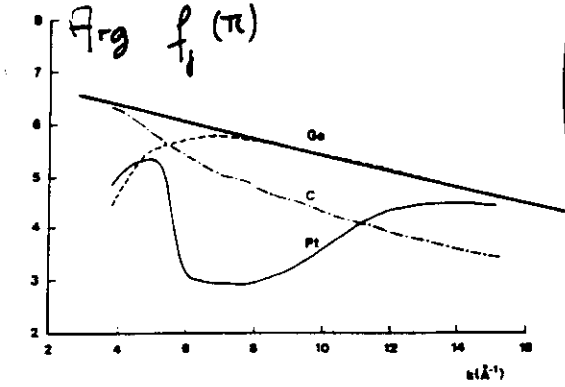

(a)

θ_j

average slope

-0.15 Å

$\frac{d\theta_j}{d(2k)} \sim 0.05$ Å

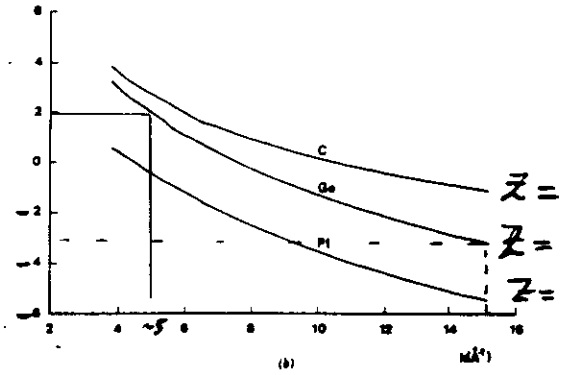

(b)

ure 6.5. (a) Theoretical scattering phase shifts for carbon, germanium, and platinum versus k. Theoretical central atom phase shifts for carbon, germanium, and platinum. All calculations are m Teo and Lee (14).

$Z = 6$ C

$Z = 32$ Ge

$Z = 78$ Pt

$2\delta_1$

$\left\langle \frac{1}{2}\frac{d(2\delta_1)}{dk} \right\rangle = -\frac{0.5}{2}$ Å

Phase $= 2kR_j + 2\delta_1(k) + \theta(k)$ $\Rightarrow$ VERY GOOD EVALUATION

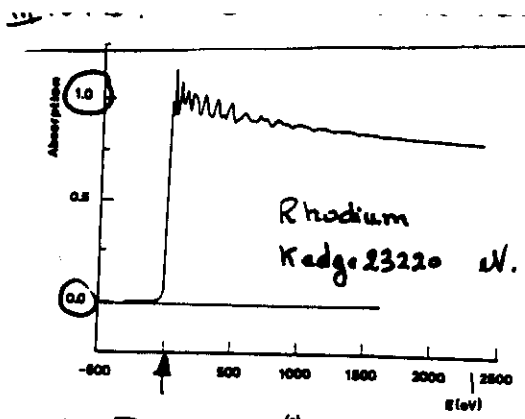

(c)

PRE-EDGE REMOVAL + NORMALISATION

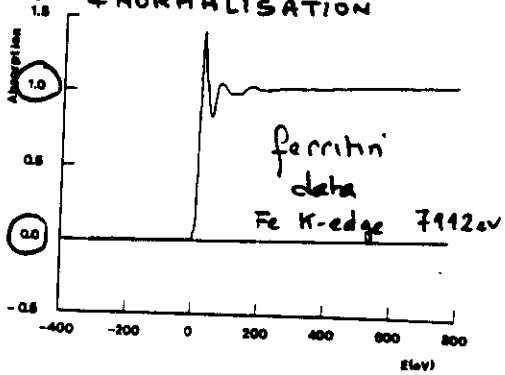

(d)

Figure 6.1. (Continued)

3 Choice of E_0 as the inflection point.

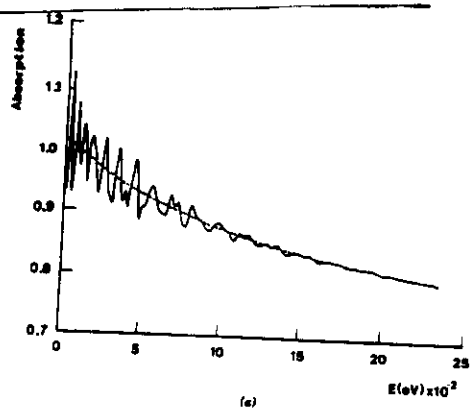

(a)

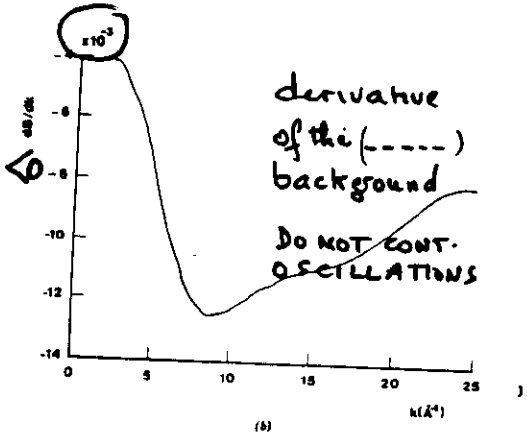

(b)

Figure 6.2. (a) The normalized data of Fig. 6.1c for rhodium metal showing on an expanded scale for the data above the edge. The calculated background curve used to extract the EXAFS is shown as a dashed line. (b) The derivative of this background curve versus the photoelectron wave vector k. (c) The normalized EXAFS for rhodium metal plotted versus k.

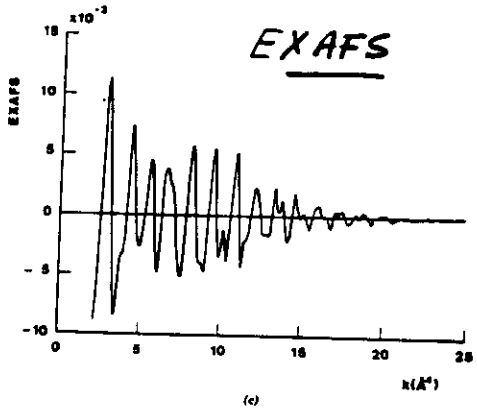

(c)

Figure 6.2. (Continued)

D. SAYERS, B.A. BUNKER

Ch 6 · EL Koningsberger, Zinn

... of evaluation of accuracy:
in R, N determinations in the best conditions
for both experiment & data handling

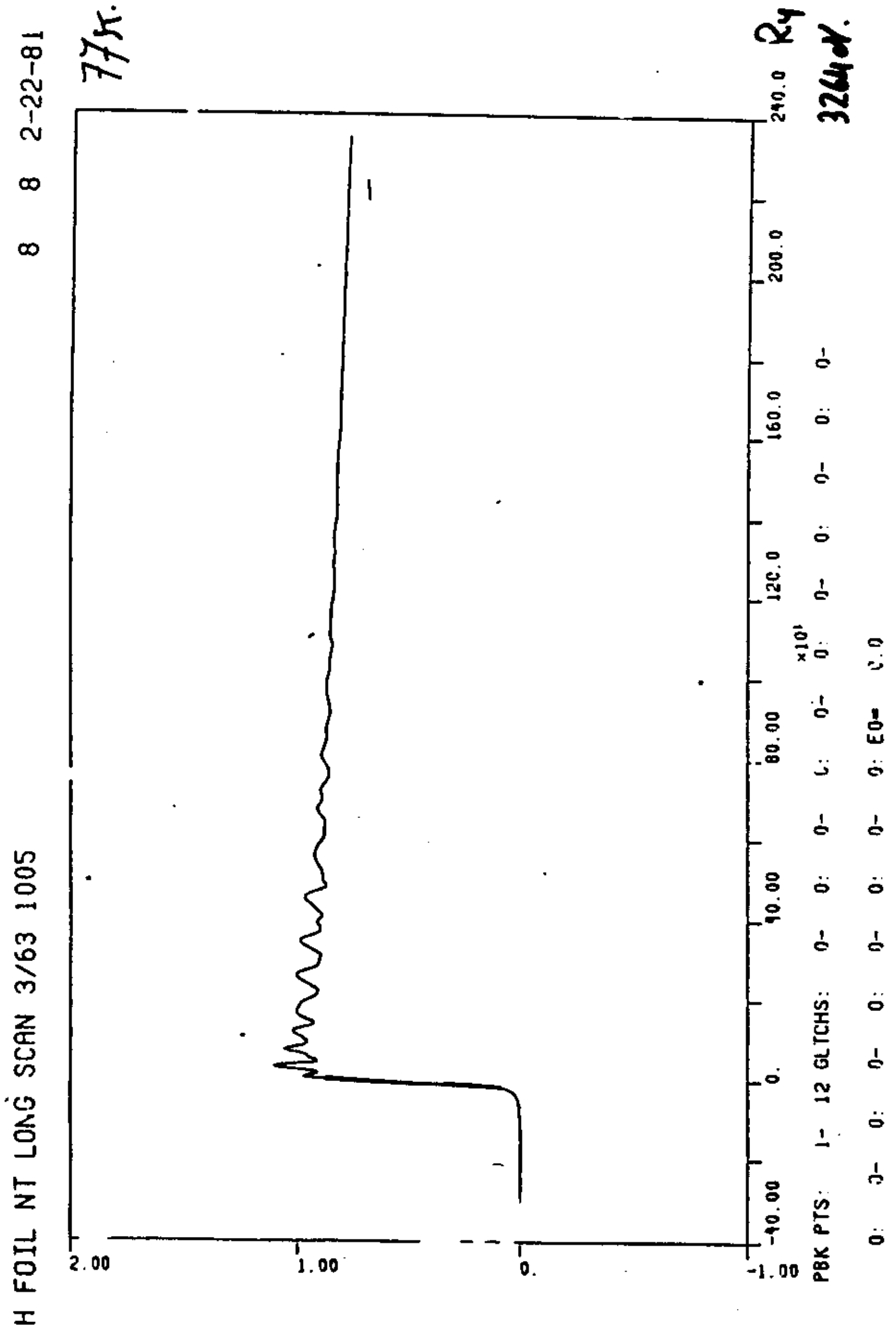

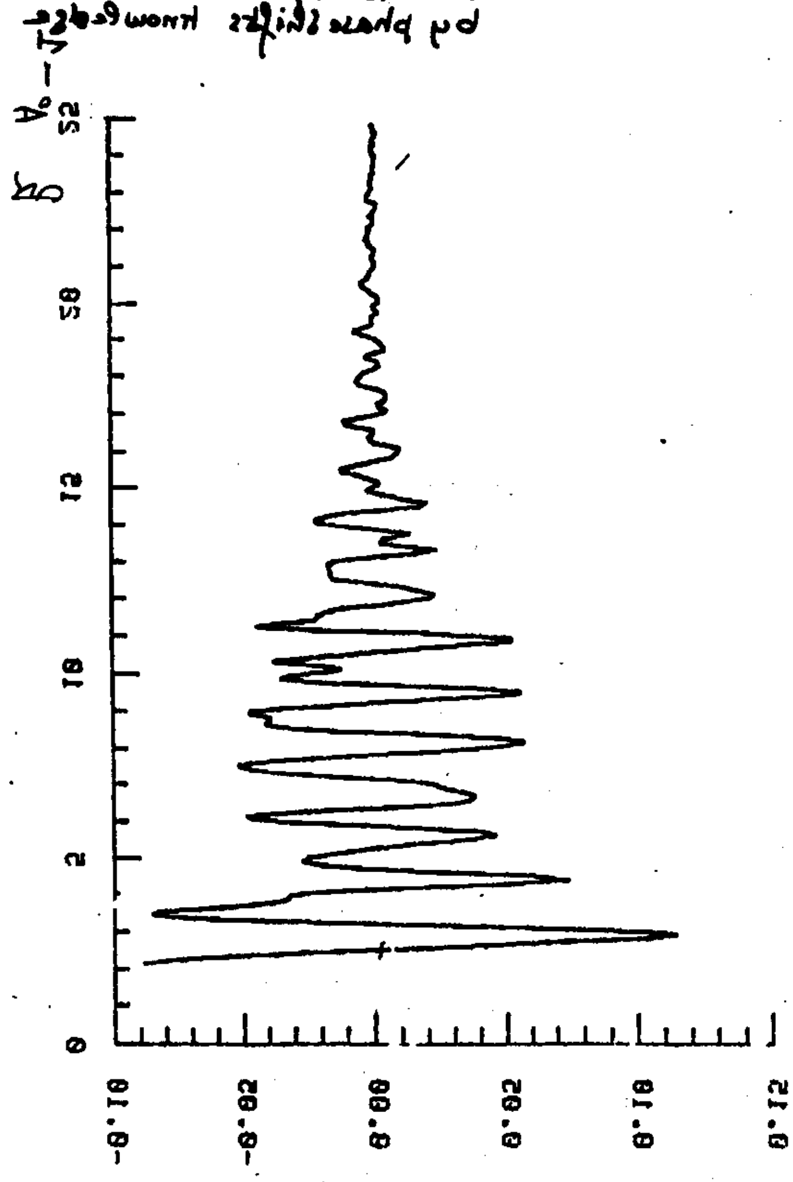

III.5d

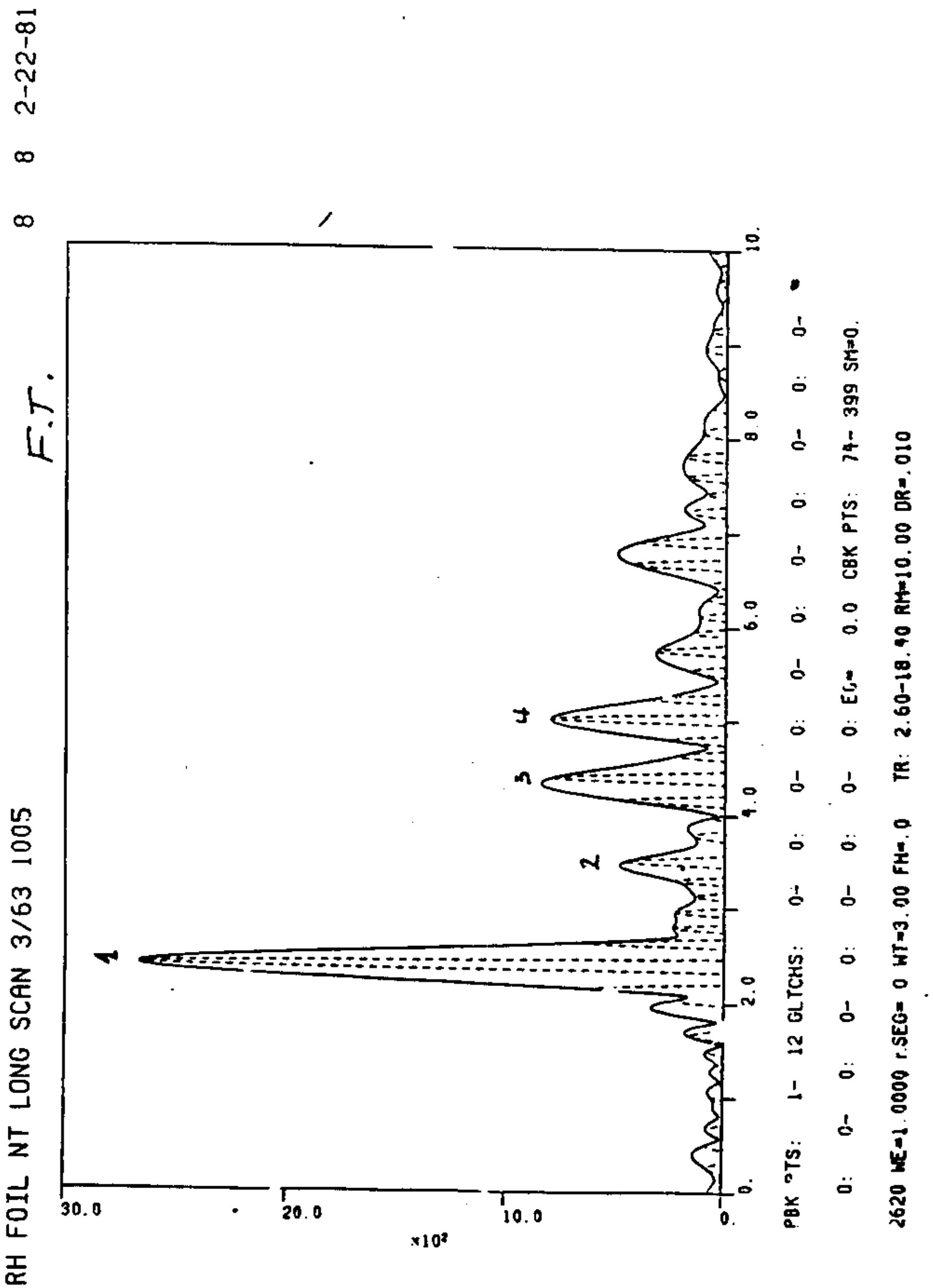

Rhodium Foil. (fcc) (Data SSRL line I 5 Feb 81.)

D. SAYERS. NCSU.

MODEL → Phase shift & Amplitude

shell #	k-range	λ	N	R	$\Delta\sigma^2 \times 10^4$ Å²	E_0(eV)
1 (MODEL)	5 - 17	λ_1	12	2.69	2.23	-.24
1	6 - 16	"	11.8	2.69	2.13	.42
2	5 - 17	"	4.77	3.80	1.96	-.06
2	6 - 16	"	4.78	3.80	1.97	-.24
3	5 - 17	"	24.7	4.67	3.12	-.4
3	6 - 16	"	25.1	4.67	3.21	-.4
4	5 - 17	"	12.1	5.38	3.14	+.4
4	6 - 16	"	12.78	5.38	3.38	+.2

k-range in $Å^{-1}$

$$\chi(k) = \sum_j \frac{N_j}{kR^2} e^{-2\sigma^2 k^2} e^{-\frac{R}{\lambda}} \left| f_j(\pi, k) \right| \sin(2kR + \psi)$$

$$\psi = 2\delta + \mathrm{Arg}\left[f_j(\pi, k) \right]$$

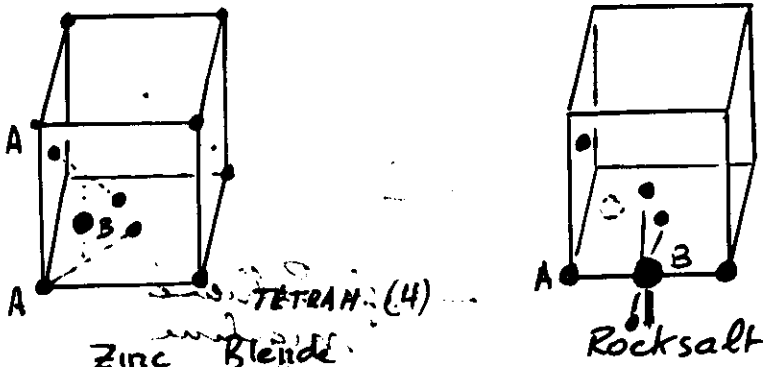

- Departure of $f_j(\pi, k)$ from atomic-like behavior
  - NON SPHERICITY of the atomic potential
  - Electrons on the A-B bond

- Smaller HP Cell. GO TO A LARGER Number of LOW Z el^{ts}

X-ray absorption spectroscopy at high pressures

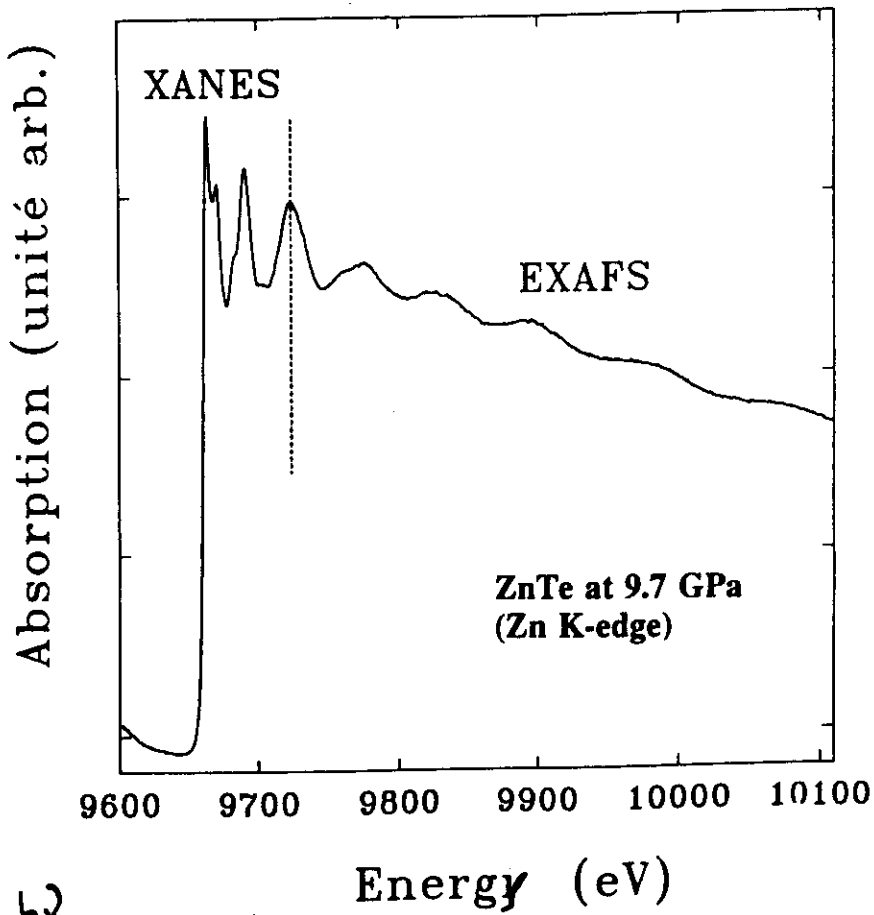

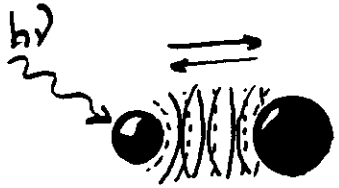

Simple "model"

$$\chi(k) = \sum_i \frac{N_i}{k R_i^2} A_i(k) \sin(2kR_i + \phi_i(k)) e^{-2k^2\sigma_i^2} e^{-\frac{2R_i}{\lambda(k)}}$$

Zn - Se under high pressure

EXAFS spectra

Zn Se p=0

EXAFS ANAL.

PHASE SHIFTS ϕ_{Zn-Se} ϕ_{Se-Zn}

&

AMPLITUDE A_{Zn-Se} A_{Se-Zn}

Zn - Se p↑

FITTING ROUTINE

R_j

N_j

$\Delta\sigma_j^2$

Local Environment

Pressure-dependent EXAFS

~ Perturbative Approach.

Zinc. Blende ⟶ (11 GPa) Rocksalt

A. San Miguel
Thesis June 1993

ZnSe

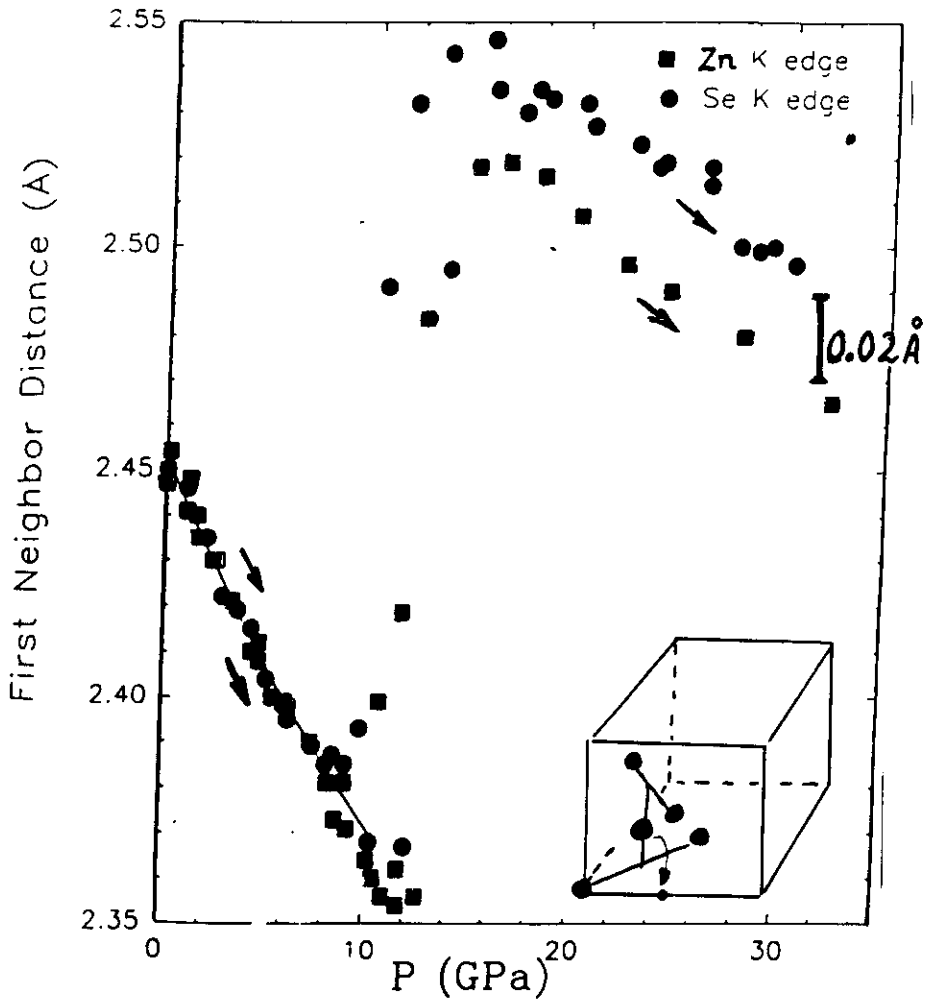

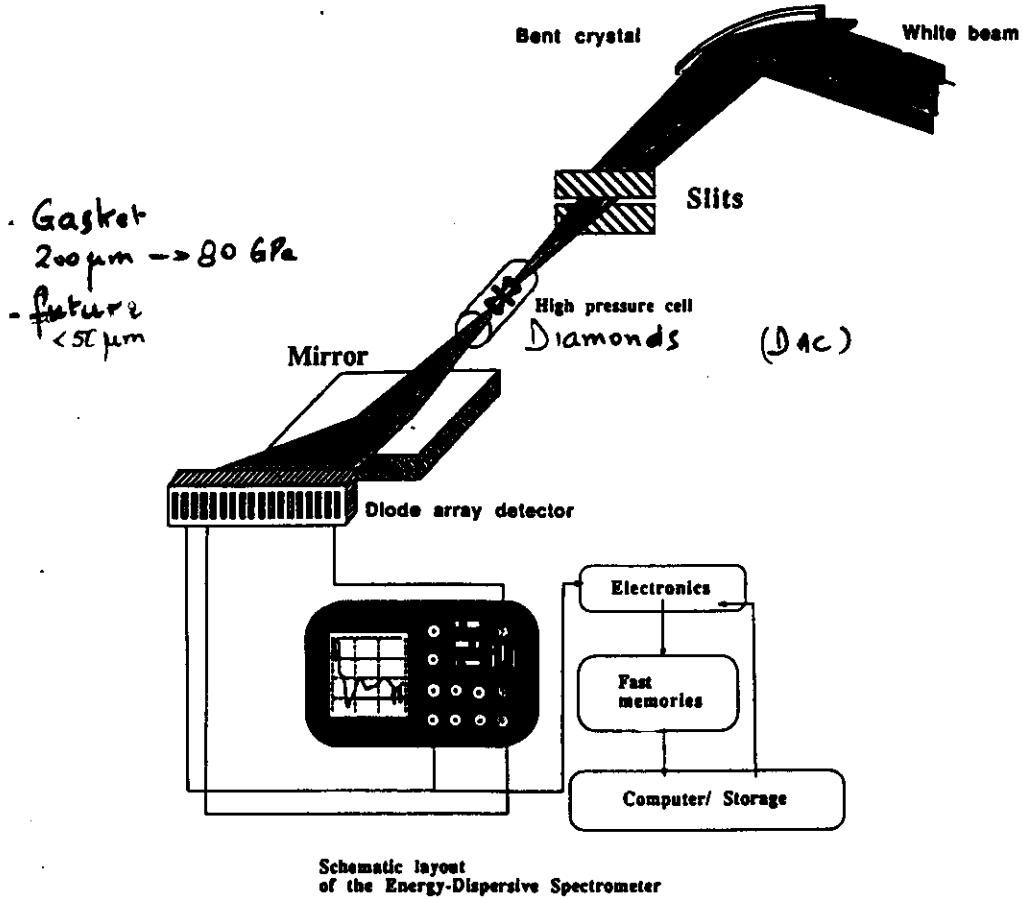

Schematic layout
of the Energy-Dispersive Spectrometer

- Gasket
  200 μm -> 80 GPa
- future
  < 50 μm

(DAC)

)VANTAGES for high pressure experiments:

'ocusing optics

.ack of mechanical movement

)irect visualization

Domain of energy: 250 - 700 eV above the edge

FIRST NEIGHBOR DISTANCE DETERMINATION
Absolute resolution: ~ 0.5 - 1 %
Relative resolution: 0.1 - 0.2 %

$$\chi(k,T) = \frac{1}{k} S_0^2(k) A(k) \int_{\text{ONE SHELL}} \frac{\rho(T,r)}{r^2} \exp -\frac{2r}{\lambda} \sin(2kr + \phi(k))\, dr$$

$$R(T) = \langle r \rangle = \frac{1}{N} \int r\, \rho(T,r)\, dr$$

$$\sigma^2(T) = \langle (r - R(T))^2 \rangle_T$$

$$C_3(T) = \langle (r - R(T))^3 \rangle_T$$

$$\boxed{\chi(k,T) = \mathcal{A}(k,T) \sin \Psi(k,T)}$$

$$\mathcal{A}(k,T) = S_0^2 \frac{A}{R^2} N \exp -2\frac{R}{\lambda} \exp[-2\sigma^2 k^2]$$

$$\Psi(k,T) = 2k\left[R - \sigma^2\left(\frac{1}{R} + \frac{2}{\lambda}\right)\right] - \frac{4}{3} C_3 k^3 + \phi(k)$$

($T \ll \Theta_D$; $C_3 k^3$; $\phi(k)$)

- $\phi(k)$
- S_0^2 MANY BODY EFFECTS

0.7 -> 0.9

$$|i\rangle = \varphi_{1s^2}\, \varphi_{2s^2}\, \varphi_{2p^6} \ldots\ldots$$

$$|f\rangle = \varphi^*_{1s^1}\, \varphi'_{2s^2}\, \varphi^*_{2p^6} \ldots\ldots$$

$$\langle \varphi_{2s^2} / \varphi'_{2s^2} \rangle \lesssim 1$$